Body Waveform Modeling of Five Moderately Earthquakes in the Zagros Fold Thrust Belt

Mehrdad Mostafazadeh[1], Omer Alptekin[2] and Ali Osman Oncel[3]

1. Assistant Prof., Seismology Research Center, International Institute of Earthquake Engineering and Seismology, P.O. Box 19395/3913, Tehran, Islamic Republic of Iran, email: mehrdad@dena.iiees.ac.ir

2. Professor of Seismology, Department of Geophysics, Istanbul University 34850 Avcilar, Istanbul, Turkey, email: alptekin@istanbul.edu.tr

3. Assistant Prof., Department of Geophysics, Istanbul University, 34850 Avcilar, Istanbul, Turkey, email: oncel@hotmail.com

ABSTRACT: *The generalized linear inverse technique has been applied to the problem of determining earthquake source models for five moderately large earthquakes in the Zagros Fold Thrust Belt (ZFTB). These earthquakes occurred in the southeastern (29 April 1987, m_b=5.9, 12 July 1983, m_b=5.8), central (12 July 1986, m_b=5.6), northwestern (28 May 1983, m_b=5.1, 18 December 1980, m_b=5.8) parts of the ZFTB. Propagation and instrumental effects are deconvolved from the long period P and SH wave records of GDSN stations to obtain the teleseismic source time function using a damped least squares inversion. The inversion has the additional constraint that the source time function is positive everywhere. A comparison of source time function of these events show that the average source duration of earthquake along the strike-slip Kazerun fault is greater than the other parts of the region. Generally slow earthquakes have long source duration. Slow risetime presumably results from a very low stress drop. Focal mechanisms of the earthquakes are thrust in the southeastern ZFTB, and have strike-slip components in the central and northwestern ZFTB. Depth values of these events are estimated to vary between 5-15km. Considering the depths and observed emergent moment release, we speculate that these events occurred beneath the sedimentary sections near to the detachment horizon. The slip vectors along the Zagros zone that are computed on the basis of compiled focal mechanism solutions in this and previous studies show a similarity with direction of convergence between the Arabian plate and the Iranian plateau.*

Keywords: Centroid depth; Earthquakes; Waveform modeling; Iran; Bitlis Zagros

Introduction

The Zagros Fold-Thrust Belt (ZFTB) is a collision zone, which is formed due to the northeast motion of the Arabian plate toward the central plateau of Iran. This belt extends to Bitlis suture zone in Southeastern Turkey [1] as shown in Figure (1).

One of the most powerful tools for better understanding of deformation in continental collision zones is to study the process of faulting in the crust along the boundary of plates. Some researchers used plate tectonics theory and introduced different tectonic zonation maps for the Iranian plateau [2, 3]. The essential database in these models are the focal mechanism solutions, slip vectors mainly determined from P wave first motions, and correlation of epicenters with geological structures. McKenzie [4] showed that present deformation is occurring as the result of small continental plates moving away along the Zagros and east Anatolian block. McKenzie [4] also showed that the earthquakes in the folded foothills of Zagros are predominantly thrust faulting, but depending on the assumed crustal velocity, many have strike-slip components. In addition, he believed that the seismic trends are not clearly related to surface faults. The difference between these models can be observed clearly. For example, the Lut block in the tectonic map of Nowroozi [2] is not shown by McKenzie [4] and Dewey [3], or the eastern plate boundary in the map of McKenzie [4] is not shown by Dewey [3]. In addition, we can see the lack of harmony between slip vectors for the same block in these classifications. Only Nowroozi [5] introduced microzonations map for the entire Iranian plateau.
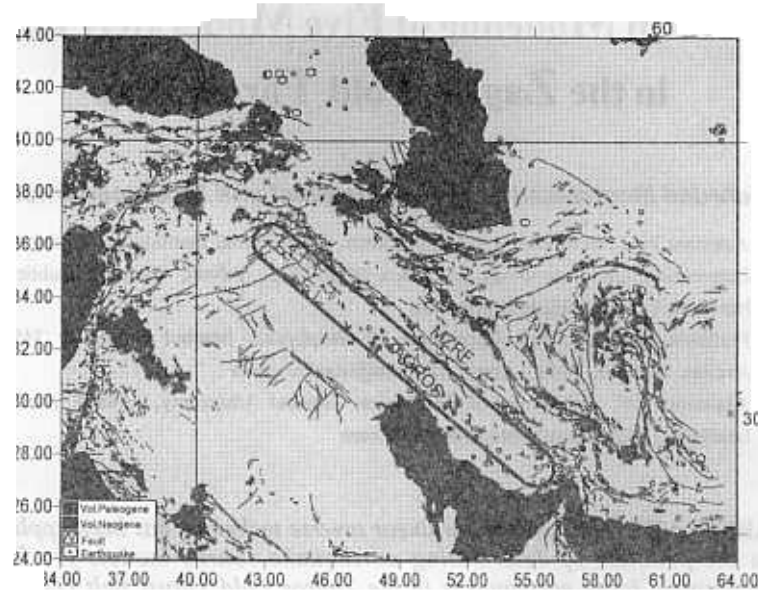
Figure 1. Tectonic and seismicity map of Iran and neighborhood area.

Seismic body waves are extensively used to determine the rupture pattern of earthquakes. The rupture pattern is generally very complex, and the results are interpreted in terms of a distribution of "asperities" and "barriers" on the fault plane. The asperity model assumes that the earthquake fault consists of several strong, highly stressed regions surrounded by an essentially stress free area [6]. The barrier model assumes that the earthquake fault consists of several fractures separated by strong barriers which remain unbroken after the event [7]. The rupture pattern is important for an understanding of the mechanism of rupture initiation and excitation of strong ground motion [8]. For example in the inversion method of Nabelek [9], the mechanism of subevents is determined by an iterative least-square method. Baker and Langstone [10] developed a generalized inverse technique utilizing the moment tensor formalism. Koyama [11] inverted teleseismic long-period body waves to a time sequence of moment tensors. Hirata and Kawasaki [12] analyzed body waves from a deep earthquake and investigated the change in the fault mechanism during the source process. In this paper, waveform modeling is used to determine faulting process along the different segments of the ZFTB.

2. The Zagros Zone

The Zagros mountains contain a thick, almost continuous sequence of shelf sediments from Paleozoic to Late Tertiary age, deposited over the Infra-Camberian Hormoz Salt Formation, which itself maybe a km or more thick [13]. This sequence is distinct from the rocks of central Iran, and is separated from them by a structure called the Zagros Thrust line that marks the NE boundary of the Zagros [14]. In the Late Cretaceous, ophiolitic-like rocks were emplaced along the NE margin of the Zagros, indicating that some shortening occurred then. However, most of the width of

the Zagros is occupied by what is known as the "Simple Folded Belt" which contains the thick Palezoic-Mesozoic-Tertiary shelf deposits that were warped into elongate, open folds in the Miocene onwards [15].

The Zagros Fold-Thrust Belt (ZFTB) is represented by five morphotectonic units based on the data from structural geology, morphology and seismicity. These are the High Zagros Thrust Belt (HZTB), Simple Folded Belt (SFB), Zagros Foredeep (ZFD), Zagros Coastal Plane (ZCP), and the Persian Gulf. The transcending boundaries between these units are called as master "blind" thrust faults: Main Zagros Reverse Fault (MZRF), High Zagros Fault (HZF), Mountain Front Fault (MFF) and Zagros Foredeep Fault (ZFF) respectively, see Figures (2, 5, 8) [16]. The thickness of the sedimentary cover and the crust in ZFTB are suggested to change from 12-14km [17, 18, 19] and 40-45km respectively [20]. Generally the simple fold belt has NW-SE trending but it changes to E-W direction in the southeast of the region [16]. The Main Zagros Reverse Fault (MZRF) has a NW strike from western Iran to the north of Bandar Abbas, where it changes to a N-S trend in Minab [16]. The ZFTB shows a high degree of seismic activity associated with complex faulting composed of generally high angle reverse and rarely vertical dip slip faults [21]. Earthquakes occur throughout the 200-300km width of the Zagros mountains, along the Zagros Thrust line. However, except in the NW of the belt, most of the larger ($m_b \geq 5.0$) earthquakes in the Zagros occur along its SW front, between the coast of the Persian Gulf and the 1500m topographic contour [21, 22].

3. Long-Period Waveform Modeling

Body waveform modeling has become one of the most important tools available to seismologists for better understanding the structure models and identifying
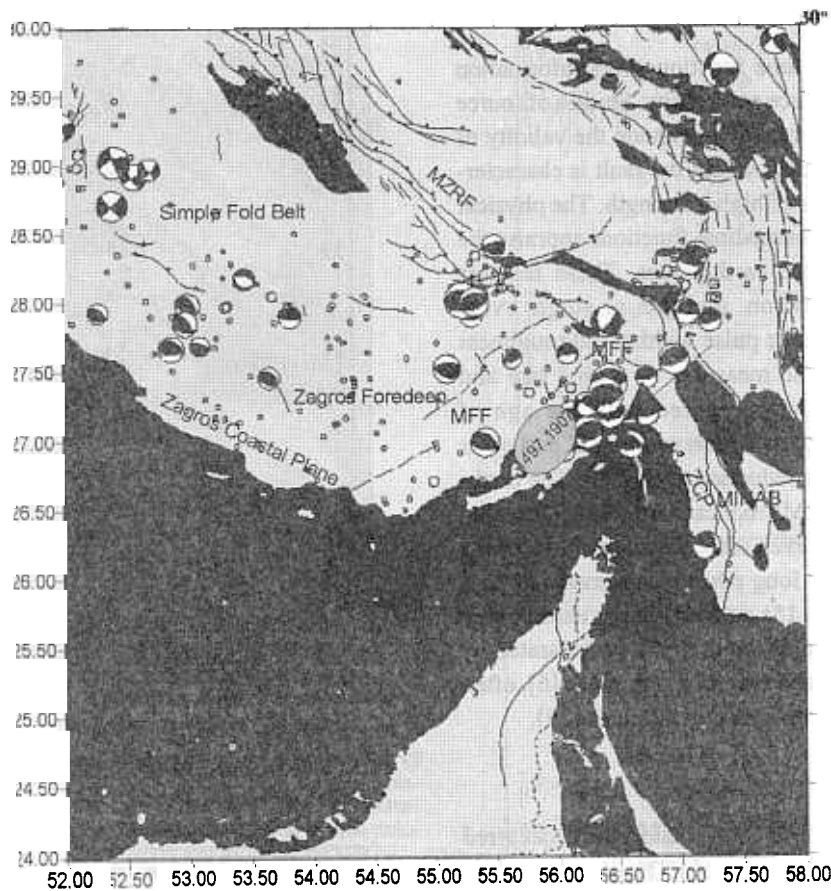
Figure 2. Tectonic and seismicity map of southeast part of the ZFTB. The locations of 12.07.1983, 29.04.1987 and historical events are shown in this map. Focal mechanisms corresponding to the best double couple solutions of the CMT inversion is reported by USGS.

fault-rupturing process. Three component waveform data from the far-field GDSN stations were obtained for the selected earthquakes. IASPEI SYN4 algorithm [23], which is a recent version of Nabelek's [9] inversion procedure based on a weighted least squares method, was used for waveform inversion. The source time function (described by a series of overlapping isosceles triangles [23]), centroid depth, and the fault orientation parameters (strike, dip, and the rake) are used in order to compute synthetic seismograms and the seismic moment.

The inversion procedure adjusts the relative amplitudes of the source time function element, the centroid depth, the seismic moment and source orientation. We refer to this solution as the minimum misfit solution. The Green's function for P and SH waves can be expressed in [24]

$$g(t) = C^R(t) \cdot M(t) \cdot g^S(t) \qquad (1)$$

where $g^S(t)$ is the displacement of the P or SH waves emerging at the base of the crust in the source region in response to a impulse, $M(t)$ and $C^R(t)$ are the responses to these waves by the mantle and crust at the receiver respectively.

Amplitudes are corrected for geometrical spreading and attenuation is introduced with a $t^* = 1s$ for P wave and $t^* = 4s$ for SH wave [9]. As explained by Fredrick [25],

uncertainties lie in t^* effect mainly the source duration and seismic moment, rather than the source orientation or centroid depth.

The seismic moment clearly depends on the duration of the source time function, and to some extends on centroid depth and velocity structure [24]. As our main interest is in source orientation and depth, we did not concern ourselves much with uncertainties in seismic moment, which in most cases are probably about 30 per cent. We estimated the lengths of time functions by increasing the number of isosceles triangles until the amplitudes of the later ones became insignificant.

Having found a set of acceptable source parameters, we followed the procedure described by MaCaffrey & Nabelek [26], Nelson [27], Fredrick [25], in which the inversion routine is used to carry out experiments for testing how well individual source parameters are resolved. We investigated one parameter at a time by fixing it at a series of values either side of its value yielded by the minimum misfit solution, and allowing the other parameters to be found by the inversion routine. We then visually examined the quality of fit between observed and synthetic seismograms to see whether it had deteriorated from the minimum misfit solution. In this way we were able to estimate the uncertainty in strike, dip, rake and depth for each event.

4. Source Time Function

The teleseismic source time function gives information about fault rupture or source complexity. Studies of source complexity are also important to evaluate the validity of asperity models of faulting, where the fault is characterized by localized regions of higher strength. The physical features of teleseismic source time functions appraise the source complexity of the earthquakes. These features include the overall duration, multiple or single event character, individual source pulse widths, and roughness of the time function. The measures of source size and complexity can then be compared with the age of subducted lithosphere, plate convergence rate, and other physical parameters of subduction zone [28]. The earthquakes larger than about Ms>6.9 can rarely be represented by a single point source, even at the wavelengths recorded by the WWSSN 15-100 long period instruments (with a peak response at a bout 15s period). These earthquakes usually consist of several discrete ruptures, separated by several seconds in time and several km in space [6], often occurring on faults with different orientations [29].

5. Results

The 12 July 1983 and 29 May 1987 main-shocks occurred in the southeast of the Zagros Fold-Thrust Belt near to Mountain Front Fault (MFF), see Figure (2) (four after-shocks were reported for these earthquakes by USGS). The historical (1497, M=6.5 and 1907, M=5.7) and instrumental earthquakes (1.4.1947 main shock M=7.0 and 21.03. 1947 foreshock) show that this area has large potential for occurrence of destructive earthquakes. In our model, the nodal plane 1 is the fault plane. Number of source time function element is $N_T = 2$ for July 1983 earthquake and $N_T = 1$ for May 1987 earthquake. Source time functions of these earthquakes are 4 and 3.1 seconds. Mechanisms of these earthquakes are pure thrust with little strike component faulting, see Figures (3, 4).

The Kazerun fault is one of the most important tectonic units in ZFTB, see Figure (5). Some of the historical earthquakes (1824 and 1891 earthquakes) are reported near to this fault [16]. The epicenter of 12 July 1986 main-shock in the Zagros Fold Belt is near to this fault (three aftershocks were reported by USGS). Baker et al [30] calculated centroid depths of some moderately strong earthquakes that occurred along the Kazerun fault. They suggested that the majority of these earthquakes are in metamorphic basement. In our model, we select a half duration time of $\tau = 0.78\ sec$ for this event. The structural model beneath the stations is a half space and P and SH wave velocities are $V_P = 6.4km/sec$ and $V_S = 4.1km/sec$ respectively. Focal mechanism of this event describes strike-slip faulting, see Figure (6). The epicenter of 28 May 1983 main-shock in the regional saddles in the Zagros Foredeep, namely Dezful Embayment (DE), see Figure (5) (five aftershocks were reported for this event by USGS). In
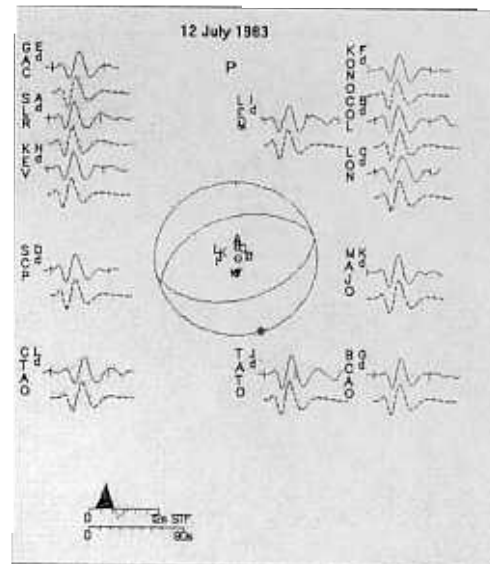

Figure 3. The P radiation patterns of minimum misfit solutions for the earthquake of 12.07.1983 main shock, observed waveform (upper trace), synthetic data (lower trace), and source time function are shown in this figure. The P and T axes are marked by solid open circle, respectively. The station code is identified to the left of each waveforms, and lower case letter that indicates the type of instrument (d = GDSN long period).
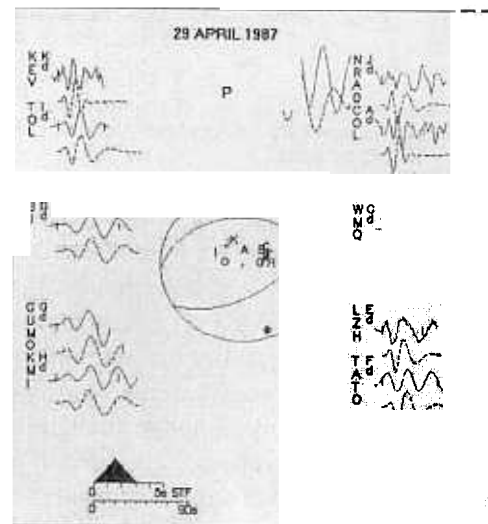

Figure 4. The P radiation patterns of minimum misfit solutions for the earthquake of 29.04.1987 main shock are shown in this figure. Observed waveform (upper trace), synthetic data (lower trace), and source time function are also shown in this figure. The P and T axes are marked by solid and open circle, respectively. The station code is identified to the left of each waveforms, and lower case letter that indicates the type of instrument (d=GDSN long period).

our model, the number of source time function is $N_T = 2$ and half duration time is $\tau = 0.95sec$. A two layered structural model with P and SH waves velocities of 5.3-6.9km/sec and 3.4-4.5 km/sec are used. The mechanism of this earthquake as determined from the inversion is reversed with strike-slip component, see Figure (7).

The 18 December 1980 main-shock occurred in north-west of the ZFTB, see Figure (8) (two aftershocks were

Figure 5. Tectonic and seismicity map of the central part of ZFTB. The location of 12.07.1986, 28.05.1983 and historical events are shown in this map. Focal mechanisms corresponding to the best double couple solutions of the CMT inversions are reported by USGS.

Figure 6. The P and SH radiation patterns of minimum misfit solutions for the earthquakes of 12.07.1986 main shock are shown in this figure. Observed waveform (upper trace), synthetic data (lower trace), and source time function are also shown in this figure. The P and T axes are marked by solid and open circle, respectively. The station code is identified to the left of each waveforms, and lower case letter that indicates the type of instrument (d=GDSN long period).

Figure 7. The P and SH radiation patterns of minimum misfit solutions for the earthquake of 28.05.1983 main shock are shown in this figure. Observed waveform (upper trace), synthetic data (lower trace), and source time function are also shown in this figure. The P and T axes are marked by solid and open circle, respectively. The station code is identified to the left of each waveforms, and lower case letter that indicates the type of instrument (d=GDSN long period).

Figure 8. Tectonic and seismicity map of northwest part of the ZFTB. The location of 18.12.1980 and historical events are shown in this map. Focal mechanisms corresponding to the best double couple solutions of the CMT inversions are reported by USGS.

reported for this event by USGS). Some historical earthquakes (628, 1179, 1573 and 1714 earthquakes) are reported near this area [16]. In our model we used a number of source time function element $N_T = 1$ with a half duration $\tau = 1.2 sec$. A structural model with two layers with P and SH waves velocities between 4.4-6.9km/sec and 2.5-4.4km/sec is used in the inversion respectively. The mechanism of this earthquake as determined from the inversion is reversed with strike-slip, see Figure (9).
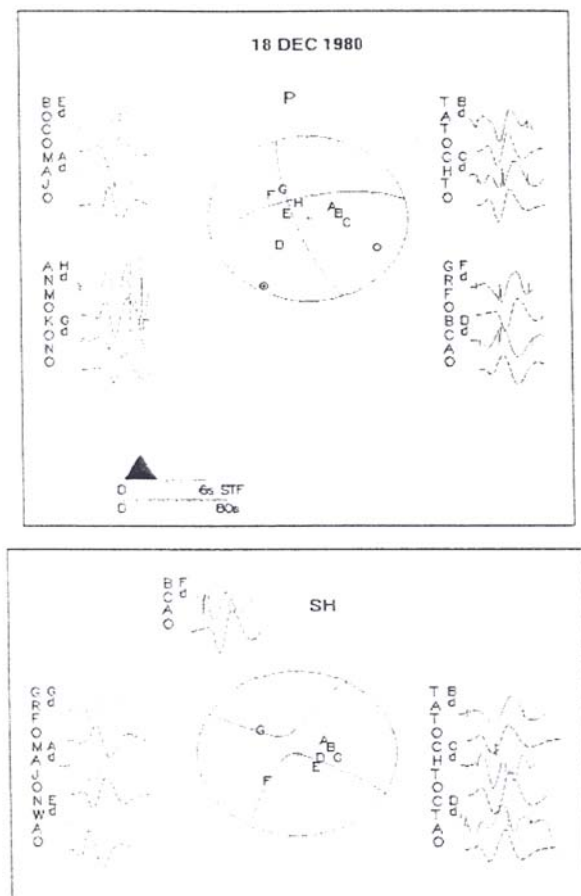
Table 1. Source time function of earthquakes that were studied by waveform inversion. TS (This Study), NB (Ni and Barazangi, 1986), BJP (Baker, Jackson and Priestley, 1993).

Date	Lat.	Lon.	Source Time Function (Sec.)	Ref.
24.03.1963	34.44	47.80	1.7	NB
11.01.1967	34.09	45.67	1.2	NB
12.06.1927	32.98	46.25	1.2	NB
22.04.1976	28.71	52.12	2.0	NB
18.10.1966	27.87	54.30	2.0	NB
08.11.1971	27.04	54.47	1.2	NB
23.02.1970	27.83	54.52	1.2	NB
19.10.1977	27.80	54.90	1.2	NB
07.02.1983	26.83	57.56	3.2	NB
21.06.1965	28.12	55.89	2.5	NB
12.04.1971	28.30	55.89	3.0	NB
06.12.1988	29.44	51.65	3.0	BJP
23.06.1968	29.81	51.16	5.0	BJP
22.04.1976	28.71	52.12	2.0	BJP
12.07.1986	29.96	51.58	1.0	BJP
20.12.1986	29.98	51.62	2.0	BJP
11.08.1988	29.97	51.57	2.0	BJP
11.08.1988	29.97	51.67	3.0	BJP
12.07.1983	27.60	56.38	4.0	TS
29.04.1987	27.39	56.07	2.0	TS
12.07.1986	29.96	51.58	2.4	TS
28.05.1983	32.59	48.53	4.0	TS
18.12.1980	36.00	44.67	2.0	TS

Figure 9. The P and SH radiation patterns of minimum misfit solutions for the earthquake of 18.12.1980 main shock are shown in this figure. Observed waveform (upper trace), synthetic data (lower trace), and source time function are also shown in this figure. The P and T axes are marked by solid and open circle, respectively. The station code is identified to the left of each waveforms, and lower case letter that indicates the type of instrument (d=GDSN long period).

6. Discussion and Conclusion

The most important new results of the study demonstrated the source time function of earthquakes along the ZFTB. A comparison of source time function of these events show that average source duration of earthquake along the strike-slip Kazerun fault is greater than other parts of the region, see Table (1). Generally slow earthquakes have long source duration. Slow risetime presumably results from a very low stress drop. The source time function of these earthquakes show that the faulting in the ZFTB consists of several fractures separated by strong barriers,

which remained unbroken after the event. If the barriers are completely broken, there may be no aftershocks within the main-shock fault plane. These results may be due to the non-homogeneity of material strength along the plane of rupture. There was no reported fresh faulting associated with these events. Considering the depths and observed emergent moment release, we speculate that these events occurred beneath the sedimentary sections near to detachment horizon.

A comparison of seismicity in different segments of the ZFTB show that continuing fracturing and energy release in SW of the region are dominant. For this reason, the possibility of occurrence of large and destructive M>7 earthquakes in this area is lower than that in other parts of the ZFTB. We complied fault plane solutions of previous earthquakes, see Table (2) that were solved by waveform modeling. These solutions and the solutions determined in this study are plotted in Figure (10), see Table (3). We can see from Figure (10) that the thrust faulting is dominant in the ZFTB. Reverse faulting based on focal

Table 2. Source parameters and the source mechanisms of earthquakes that were studied by waveform inversion. TS (This Study), NB (Ni and Barazangi, 1986), BJP (Baker, Jakson and Priestley, 1993).

No	Date	M_b	Lat.	Lon.	Mechanism	Ref.
1	18.12.1980	5.4	36.00	44.67	Strike-Slip	TS
2	24.03.1963	5.5	34.44	47.80	"	NB
3	11.01.1967	5.6	34.09	45.67	"	NB
4	12.06.1972	5.3	32.98	46.25	Reverse	NB
5	28.05.1983	5.6	32.59	48.53	"	TS
6	06.04.1972	5.4	31.99	50.70	"	NB
7	02.07.1972	5.4	30.09	50.87	"	NB
8	23.06.1968	5.3	29.76	51.24	"	BJP
9	12.07.1986	5.7	29.96	51.58	Strike-Slip	TS
10	06.04.1971	5.2	29.80	51.91	"	BJP
11	22.04.1976	5.9	28.71	52.12	Reverse	NB
12	10.04.1972	6.1	28.43	52.82	"	BJP
13	18.10.1966	5.9	27.87	54.30	"	NB
14	08.11.1971	5.6	27.04	54.47	"	NB
15	23.02.1970	5.4	27.83	54.52	"	NB
16	24.12.1975	5.5	27.04	54.50	"	NB
17	16.03.1976	5.4	27.33	55.00	"	NB
18	19.10.1977	5.5	27.80	54.90	"	NB
19	07.02.1983	5.7	26.83	57.56	Strike-Slip	NB
20	29.04.1987	5.9	27.39	56.07	Reverse with Strike Component	TS
21	12.07.1983	5.9	27.60	56.38	Reverse	TS
22	21.06.1965	5.7	28.12	55.89	Strike-Slip	NB
23	12.04.1971	6.0	28.30	55.89	Reverse	NB

Table 3. Source parameters of earthquakes studied in this paper.

Date	18.12.80	29.04.87	12.07.86	28.05.83	12.07.83
Mb	5.9	5.9	5.7	5.6	5.9
Depth (km)	14±1 15 (CMT)	12±1 15 (CMT)	8±0.5 33 (CMT)	14±0.8 27 (CMT)	14±0.9 46 (CMT)
Srtike, deep, rake nodal plane 1	247°±2 74°±6 13°±4	247°±8 42°±2 113°±2	267°±20 70°±20 336°±24	314°±3 38°±1 113°±4	244°±15 43°±12 113°±4
Strike, deep, nodal plane 2	153°±2 78°±6	62°±8 53°±2	358°±20 86°±2	106°±3 55°±1	88°±6 53°±5
M (N.M)	$1.67*10^{16}$	$1.3*10^{18}$	$4.4*10^{17}$	$2.9*10^{17}$	$1.5*10^{18}$
CMT M (N.M)	$2.01*10^{18}$	$0.433*10^{18}$	$0.412*10^{18}$	$0.253*10^{18}$	$2.1*10^{18}$
S (km²)	63.6	106	48.18	70.80	138

mechanism solutions had more dominance in ZFTB. The slip vectors along the Zagros zone show a similarity with the direction of convergence between the Arabian plate and Iranian plateau as shown in Figure (11).
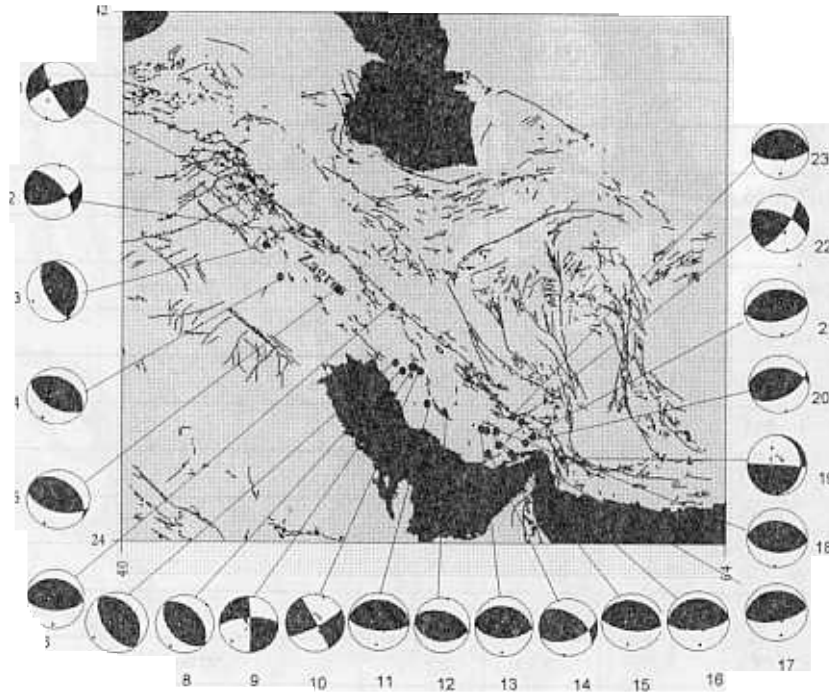
Acknowledgment

Figure 10. Focal mechanism solution of earthquakes that are used and compiled in this study.
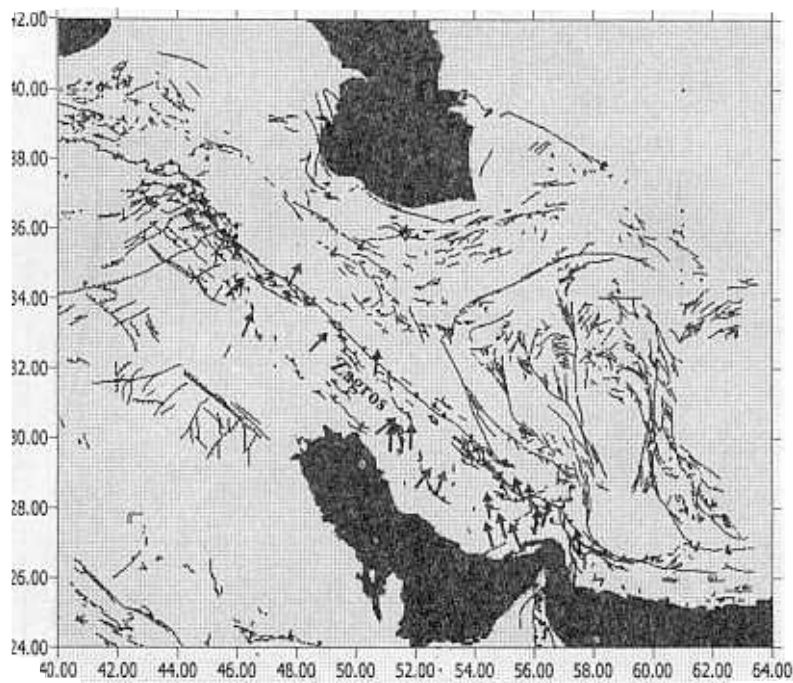

Figure 11. Horizontal projections of the slip vectors for the earthquakes that are used and compiled in this study.

References

Sengor, A.M.C. and Kid, W.S.F. (1979). "Post-Collisional Tectonics of the Turkish and Iranian Plateau and a Comparison with Tibet", *Tectonophysics*, **55**, 361-375.

2. Nowroozi, A.A. (1972). "Focal Mechanisms of Earthquakes in Persia", Turkey - West Pakistan, and Afghanistan and Plate Tectonics of the Middle East. *Bull. Seism. Soc. Am.*, **62**(3), 823-850.

Dewey, J.F., Pitman, W.D.F., and Bonnin, J. (1973). "Plate Tectonics and Evolutions of the Alppine System", *Geol, Soc. Am. Bull.*, **84**, 3138-3180.

4. McKenzie, D. (1972). "Active Tectonics of Mediterranean Region", *Geophys. J.R. Astr. Soc.*, London, **30**, 109-185.

Nowroozi, A.A. (1976). "Seismotectonics Province of Iran", *Bull. Seism. Soc. Am.*, **66**(4), 1249-1276.

6. Kanamori, H. and Stewart, G.S. (1978). "Seismological Aspects of the Guatemala Earthquake", *J. Geophys. Res.*, **83**, 3427-3434.

Das, S. and Aki, K. (1977). "Fault Plane with Barriers: A Versatile Earthquake Model", *J. Geophys. Res.*, **82**, 5658-5670.

8. Kikuchi, M. and Kanamori, H. (1991). "Inversion of Complex Body Waves- III", *Bull. Seism. Soc. Sm.*, **81**, 2335-2350.

9. Nabelek, J.L. (1984). "Determination of an Earthquake Source Parameters from Inversion of Body Waves", Ph.D. Thesis, MIT, Cambridge, Massachusetts.

10. Barker, J. and Langeston C.A. (1987). "Inversion of Teleseismic Body Waves for the Moment Tensor or the 1978 Thessaloniki", Greece Earthquake, *Bull. Seism. Soc. Am.*, **71**, 1423-1444.

11. Koyama, J. (1987). "Time-Dependent Moment Tensor Inversion for the 1983 Japan Sea Earthquake", Zisin 2, **40**, 405-416 (in Japanese with English abstract).

12. Hirata, K. and Kawasaki, I. (1988). "Space Time Dependent Moment Tensor", *Program and Abstracts Seism. Soc.*, Japan, **2**, 16, (in Japanese).

13. Berberian, M. and King, G. (1981). "Towards a Paleogeography and Tectonics Evolution of Iran", *Can. J. Earth Sci.*, **18**, 210-265.

14. Stocklin, J. (1974). "Possible Ancient Continental Margins in Iran", *The Geology of Continental Margins*, 873-887, Eds. Burk, C.A., and Drake, C.L., Springer, New York.

15. Falcon, N.L. (1974). "Southern Iran: Zagros Mountains", Spencer (Editor), Mesozoeic-Cenozoice Orogenic Belts, and Data for Orogenic Studies, *Geol. Soc.* London, Spec. Publ., **4**, 199-211.

16. Berberian, M. (1995). "Master Blind Thrust Faults Hidden under the Zagros Folds: Active Basement Tectonics and Surface Morphotectonics", *Tectonophysics*, **241**, 193-224.

17. James, G.S. and Wynde, J.G. (1965). "Stratigraphic Nomenclature of Iranian Oil Consortium Agreement Area", *Am. Assoc. Oet. Gol.*, **49**(12), 2182-2245.

18. Huber, H. (1997). "Geological Map of Iran, 1:1000.000 with Explanatory Notes", National Iran. Oil Company, Explore Prod. Affairs, Tehran.

19. Mostafazadeh, M. and Alptekin, O. (1994). "Using Seismic Reflections Data for Calculation of Shortening Across the Zagros Folded Belt", *10th Petroleum Congress of Turkey*, Ankara, Turkey.

20. Sobouti, F. and Arkani-Hamed, J. (1996). "Numerical Modelling of the Deformation of the Iranian Plateau", *Geophys. J. Int.*, **126**, 805-818.

21. Jackson, J. and McKenzie, D. (1984). "Active Tectonics of the Alpine-Himalayan Belt between Western Turkey and Pakistan", *Geophys. J. R. Astr. Soc.*, **77**, 185-264.

22. Ni., J. and Barazangi, M. (1986). "Seismotectonics of the Zagros Continental Collision Zone and a Comparison with the Himalayas", *J. Geophys, Res.*, **89**, 1147-1163.

23. McCaffrey, R., Abers, G., and Zwick, P. (1991). "Inversion of Teleseismic Body Waves", Digital Seismograms Analysis and Waveform Inversion, (ed. By W.H.K. Lee), IASPEI Software Library, **3**, 81-166.

24. Taymaz, T. (1990). "Earthquake Source Parameters in the Eastern Mediterranean Region, Ph.D, Thesis, Drawing College Cambridge.

25. Fredrick, J., McCaffrey, R., and Denham, D. (1988). "Source Parameters of Seven Large Australian Earthquakes Determined by Body Waveform Inversion, *Geophys. J.*, **95**, 1-13.

26. McCaffrey, R. and Nabelek, J. (1987). "Earthquakes, Gravity and Origin of the Balia Basin and Example of a Nascent Continental Fold and Thrust-Belt, *J. Geophys. Res.*, **92**, 441-460.

27. Nelson, M.R., McCaffrey, R., and Molnar, P. (1987). "Source Parameters for 11 Earthquakes in the Tien Shan", Central Asia, Determined by *P* and *SH* Waveform Inversion, *J. Geophys. Res.*, **92**, 12628-12648.

28. Hartzell, S.H. and Heaton, T.H. (1985). "Teleseismic Time Functions for Large Shallow Subduction Zone Earthquakes", *Bull. Seism. Soc. Am.*, 965-1004.

29. Butler, R., Stewart, G.S., and Kanamori, H. (1979). "The July 27 1976 Tangshan China Earthquake -A Complex Sequence of Intraplate Events", *Bull. Seism. Soc. Am.*, **69**, 207-220.

30. Baker, C., Jackson, J., and Priestley, K. (1993). "Earthquakes on the Kazerun line in the Zagros Mountains of Iran: Strike-Slip Faulting within a Fold-and-Thrust Belt, *Geophysical, J. Int.*, **115**, 41-61.